Articles

Metal-Catalyzed Radical Polyaddition for Aliphatic Polyesters via Evolution of Atom Transfer Radical Addition into Step-Growth Polymerization

Masato Mizutani, Kotaro Satoh, and Masami Kamigaito*

Department of Applied Chemistry, Graduate School of Engineering, Nagoya University, Furo-cho, Chikusa-ku, Nagoya 464-8603, Japan

Received September 11, 2008; Revised Manuscript Received November 28, 2008

ABSTRACT: The metal-catalyzed radical addition was evolved into a step-growth polymerization by using a series of designed monomers [CH_2═CH−R−OC(O)CH(CH_3)Cl] that bear a reactive C−Cl and an unconjugated C═C double bond via an ester linkage and various metal catalysts to produce novel aliphatic polyesters by the metal-catalyzed radical polyaddition. The polyaddition reactions smoothly proceeded, and the conversion reached over 99% with the $FeCl_2$/P*n*-Bu_3 or CuCl/*N*,*N*′,*N*″,*N*″′-pentamethyldiethylenetriamine system to afford the polymers in high yield. The molecular weights progressively increased with the extent of the reaction in the later stages, and the molecular weight distributions were close to 2, indicating an ideal step-growth polymerization. The well-defined polymer structures were confirmed by ^{1}H−^{1}H correlation spectroscopy NMR analysis of the products along with the model 1:1 reactions between a halide and a vinyl compound. The polyester bearing an active C−Cl terminus obtained by the radical polyaddition was employed as a macroinitiator in the metal-catalyzed living radical polymerization of vinyl monomers such as styrene, methyl methacrylate, and methyl acrylate for block copolymers consisting of polyesters and vinyl polymers.

Introduction

Developing a conceptually novel polymerization reaction is important for generating a new family of polymers in terms of their structures, properties, and functions. In particular, a novel precision polymer synthetic method is required for constructing well-defined polymers that can exert their new or enhanced properties originating from the ordered structures. Upon developing an efficient polymerization reaction, one should design or choose a highly selective and robust organic reaction as a chain-constructing reaction and efficiently build up the reactions into the polymerization for the synthesis of high-molecular-weight polymers in high yield. In addition, a versatile and widely applicable polymerization is preferable for the prospective extension of the polymerization in terms of the variety of polymer structures and properties.

Metal-catalyzed atom transfer radical addition (ATRA)[1] is one of the most highly efficient and robust carbon−carbon bond forming processes between various vinyl compounds and organic halides and is utilized for the construction of small organic molecules via inter- and intramolecular additions. This reaction is triggered by the metal-assisted homolytic cleavage of the C−X bond, followed by the formation of the carbon radical species. This then adds to the C═C double bond of the vinyl group to form the C−C bond, followed by a new C−X bond formation upon retrieving the halogen from the oxidized metal catalyst and results in the 1:1 adduct. This radical addition reaction has quite successfully been extended to chain or chain-growth radical addition polymerizations of vinyl monomers to generate and build a new category of precision polymerizations, that is, metal-catalyzed living radical polymerization or atom transfer radical polymerization (ATRP),[2−6] which permits the precise control of the polymer molecular weights for various conjugated vinyl monomers such as (meth)acrylic and styrenic monomers and enables the precision synthesis of well-defined polymers such as block,[2,3,5] end-functionalized,[2−4,7−9] graft,[3,10] star,[2,3] and more complicated polymers.[11−17] The key for the controlled radical addition polymerization lies in the highly effective and selective reversible metal-catalyzed radical-forming reaction from the carbon−halogen terminal. The carbon−halogen terminal, between the carbon adjacent to the carbonyl or the aryl group originating from the conjugated monomers and the halogen stemming from the organic halide initiator, is reactive enough for the appropriate metal complex to result in a growing carbon radical species, which then induces radical addition polymerization. However, for unconjugated monomers such as vinyl acetate and vinyl chloride, one should use a highly active metal complex, which can activate the less-reactive carbon−halogen terminal.[18,19] The judicious choice of the reaction conditions, including selections of the metal complex and the halide initiator, is thus important for the construction of a controlled/living radical addition polymerization.

We recently evolved the metal-catalyzed radical addition reaction into another step or step-growth polymerization mechanism, that is, the metal-catalyzed radical polyaddition.[20] To achieve this new process, we designed a monomer possessing a reactive C−Cl bond, which can be activated by a metal catalyst to result in the carbon radical species, and an unconjugated C═C bond, to which the resulting carbon radical can add to form a C−C bond along with an unreactive C−Cl pendant without cross-propagation via addition polymerization and polyaddition.[9] If the addition reaction can proceed intermolecularly between

* Corresponding author. E-mail: kamigait@apchem.nagoya-u.ac.jp. Fax: 81 52 789 5112.

10.1021/ma802067c CCC: $40.75
Published on Web 12/31/2008

Scheme 1. Transition-Metal-Catalyzed Radical Polyaddition of Ester-Linked Monomers

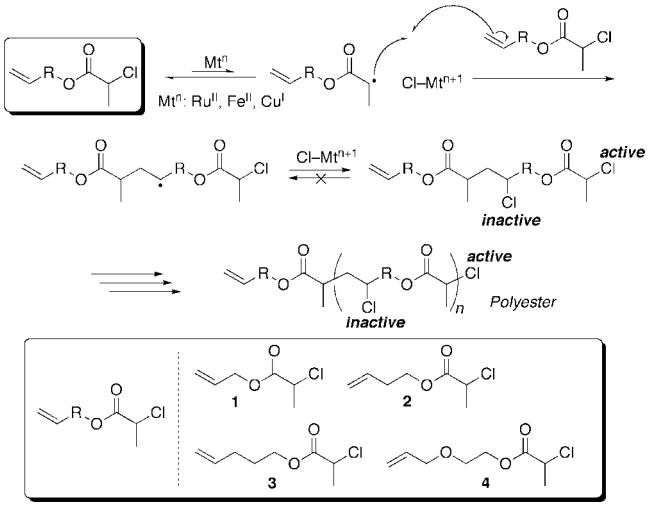

the monomers, then it will generate a dimer with one reactive C−Cl and one C═C bond at its terminal, which can be further converted stepwise into oligomers and finally linear polymers via the step-growth mechanism, whereas the analogue with a conjugated C═C bond, inimer, has been polymerized into highly branched structures regenerating reactive C−Cl bonds for cross-propagation.[11−13,21] This conceptually new radical polyaddition reaction would provide a series of novel linear polymers via the C−C bond forming reactions, in contrast with the well-known radical polyaddition with the formation of S−C bonds by thiol-ene reaction.[22] Although we have reported very preliminary results on such a metal-catalyzed radical polyaddition of certain monomers, detailed studies of the effective catalysts, mechanism, polymer properties, and applications have not yet been done.

This study is thus directed to the development and establishment of the metal-catalyzed radical polyadditions using various metal catalysts (Ru, Fe, and Cu) under different conditions for a series of monomers (**1**−**4**) possessing a C−Cl and a C═C bond linked through the ester linkage with different numbers of methylene or oxyethylene units (Scheme 1). In addition to the optimization of the reaction conditions for efficient polymerizations, the polymerization mechanisms and products were analyzed in detail using the model 1:1 reactions between a chloride and a vinyl compound and the ^{1}H−^{1}H correlation spectroscopy (COSY) NMR analysis of the products. Further studies were devoted to the application of the radical polyaddition by a combination with the metal-catalyzed living radical addition polymerization through the block copolymerization of typical vinyl monomers such as styrene, methyl methacrylate (MMA), and methyl acrylate (MA) from the polyester-type macroinitiator obtained by the radical polyaddition.

Results and Discussion

Polyaddition of Ester-Linked Monomers under Various Conditions. A series of ester-linked monomers (**1**−**4**) with an unconjugated C═C and a reactive C−Cl bond was synthesized by a simple reaction between 2-chloropropionyl chloride and the ω-alkenyl alcohols in the presence of triethylamine. Figure 1 shows the ^{1}H NMR spectra of such prepared monomers, a series of esters with α-(2-chloropropionyl) and ω-vinyl groups. Every spectrum showed a characteristic quartet at 4.4 to 4.5 ppm (*c*) assigned to the methine proton adjacent to the chlorine atom, double doublets at 5.0 to 5.3 ppm (*a*), and a multiplet at 5.8 to 6.0 ppm (*b*) of the terminal vinyl group. All of these compounds possess the 2-chloropropionyl group, which can easily generate the acryloyl radical species via cleavage of the C−Cl bond upon activation with an appropriate metal complex, and an unconjugated vinyl group, to which the radical species can add to form a stable C−Cl bond upon receiving the halogen on the resulting unconjugated unstable radical species.

These ester-linked monomers were then treated with an iron catalyst ($FeCl_2$) in the presence of tri-*n*-butylphosphine (P*n*-Bu_3) in toluene at 100 °C for the metal-catalyzed radical polyadditions. All of the monomers were smoothly consumed, and the conversion reached >90% (Figure 2A). The molecular weights of the obtained products progressively increased in the later stages of the reactions, which suggests that the polymerization proceeds via the step-growth mechanism not via the chain-growth mechanism (Figure 2B). In addition, as the polymerization proceeded, the molecular weight distributions (M_w/M_n; M_w: weight-average molecular weight, M_n: number-average molecular weight) became broader and were approaching 2.0, the theoretical value for the products obtained by the step-growth polymerization. The ^{1}H NMR spectra also showed the characteristic signals of the polymers produced via the polyaddition mechanism (Figure S1 in the Supporting Information). These results indicate that the $FeCl_2$/P*n*-Bu_3-catalyzed polymerization proceeded via an almost ideal step-growth propagation mechanism without significant intramolecular ring-closing processes. The key for the predominant intermolecular polyaddition reactions is due to the monomer structure and the relatively high monomer concentration because other α-chloro-ω-vinyl compounds undergo cyclization under diluted conditions.[23]

Figure 3 shows the size exclusion chromatograms (SECs) of the products obtained from **1**−**4** using the $FeCl_2$/P*n*-Bu_3 system. In the early stages of the reaction, the SEC curves consisted of only low-molecular-weight oligomers of which the highest peak was assumed to be that of the dimers. (See also Figure S2 in the Supporting Information.) As the reaction proceeded, the curves shifted to the high-molecular-weight region, especially after almost all of the monomers were consumed (>95%), which also indicated that the polymers were produced via a metal-catalyzed step-growth polyaddition. However, the molecular weights of the final products were around several thousand in all cases. These might be due to the lower conversions of the C═C and C−Cl groups, the side reactions between the radical species, or both, especially in the later stages of the reactions. The reaction conditions can be optimized by using other metal catalysts, changing the concentration of the monomer, catalysts, and ligands, or by changing the reaction temperatures for a higher molecular weight product.

A series of metal catalysts, which are effective for the metal-catalyzed living radical polymerization or ATRP, were then employed in the polyaddition reaction of **2**. Table 1 summarizes the monomer conversions, M_w, and M_w/M_n of the products obtained with RuCp*Cl$(PPh_3)_2$, $FeCl_2$/P*n*-Bu_3, $FeCl_2$/PCy_3, $FeCl_2$/PPh_3, $FeCl_2$/PMDETA (PMDETA/*N*,*N*′,*N*″,*N*″′-pentamethyldiethylenetriamine), CuCl/PMDETA, CuCl/bpy (bpy/2,2′-bipyridine), CuCl/Me_6TREN (Me_6TREN/tris[2-(dimethylamino)ethyl]amine), and CuCl/HMTETA (HMTETA/1,1,4,7,10,10-hexamethyltriethylenetetramine) as catalysts under various conditions.[2,3,24−27] More detailed data are plotted in Figures S3−S5 in the Supporting Information. Herein, the conversions in Table 1 and these Figures are for the monomer molecule itself but not for the functional groups such as the C═C and C−Cl bonds in the monomer units. Although the reactions were all slow, they proceeded almost quantitatively (>90%) and gave the polymers under appropriate conditions, except for RuCp*Cl$(PPh_3)_2$ (entry 1), $FeCl_2$/PMDETA (entry 2), and CuCl/bpy (entry 18). Among them, the $FeCl_2$/P*n*-Bu_3 and CuCl/

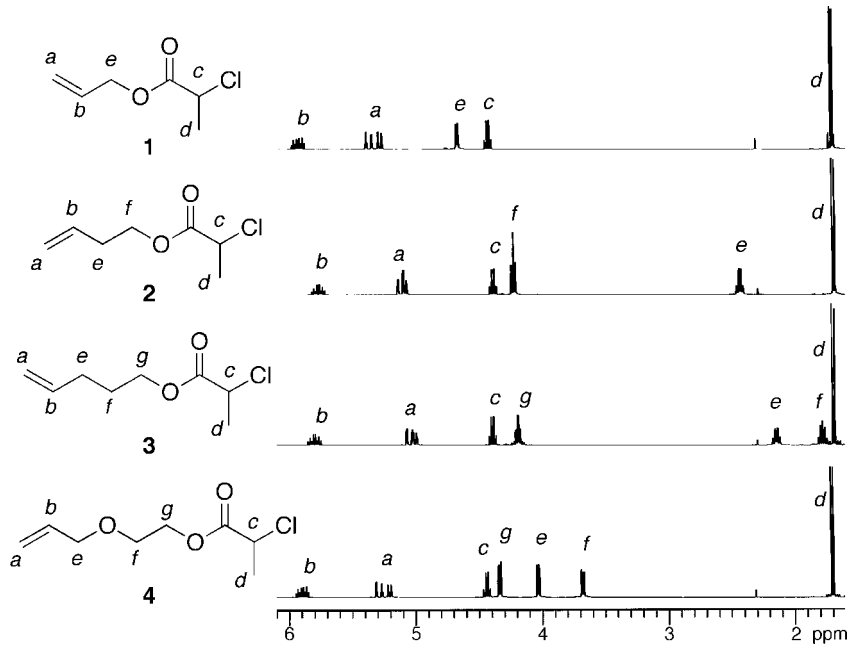

Figure 1. ^{1}H NMR spectra of the ester-linked monomers (**1**−**4**). (See Scheme 1 for structure.)

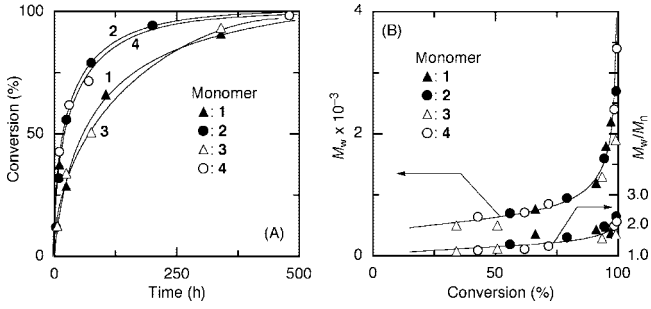

Figure 2. (A) Time−conversion and (B) conversion−weight-average molecular weight (M_w) curves for the polyaddition of **1**−**4** (Scheme 1) to $FeCl_2$/tri-*n*-butylphosphine (P*n*-Bu_3): $[monomer]_0 = 2.0$ M; $[FeCl_2]_0 = 100$ mM; $[Pn\text{-}Bu_3]_0 = 200$ mM in toluene at 100 °C. Monomer: (▲), **1**; (●), **2**; (△), **3**; (○), **4**.

PMDETA systems induced a quantitative monomer consumption (>99%) under appropriate conditions and produced polymers with relatively high molecular weights (M_w > 2500). In particular, with the $FeCl_2$/P*n*-Bu_3 system, the M_w/M_n of the polymers was close to 2, which is a theoretical value for the ideal step-growth polymerizations, indicating that the $FeCl_2$/P*n*-Bu_3 system is more suitable for the radical polyaddition of **2**.

In the polyaddition of **2**, the effects of the monomer concentration, the $[ligand]_0/[metal]_0$ ratio, and the temperature were then examined with the $FeCl_2$/P*n*-Bu_3 (entries 2−5) and CuCl/PMDETA (entries 10−15) systems. More detailed results of a series of the reactions are also shown in Figures S6−S10 in the Supporting Information. Upon increasing $[ligand]_0/[metal]_0$ to 4.0 (entry 4), the reaction became slower because the excess phosphines decreased the activity of catalysts as in the metal-catalyzed radical addition and polymerization. Upon decreasing the ratio to 1.0 (entry 2), the reaction also became slower without affecting the final molecular weights, which suggests a decrease in the concentration of a soluble complex. The best ratio of $[Pn\text{-}Bu_3]_0/[FeCl_2]_0$ was thus 2.0 (entry 3) in terms of the reaction rate and the molecular weight of the products, indicating that the effective catalyst would be the 1:2 complex of $FeCl_2(Pn\text{-}Bu_3)_2$.[25] The lower temperature resulted in a slow polymerization but was effective in producing a higher molecular weight polymer probably because of the suppression of the side reactions (entry 5). At a lower monomer concentration ($[M]_0 = 2.0$ M), the $FeCl_2$/P*n*-Bu_3 system also led to an almost quantitative conversion (99%) to give the highest molecular weight of the products among the various conditions for the iron systems (entry 6) because the relative concentration of the catalyst ($FeCl_2$/P*n*-Bu_3) to the monomer (C−Cl) increased with the lowered the monomer concentration.

Similar effects of temperature were also observed for the CuCl/PMDETA system (entries 10−13 and Figure 4). With decreasing temperature, the reaction became slower and resulted in a higher molecular weight polymer. In particular, a quantitative monomer consumption (≥99%) was achieved below 60 °C to give the highest molecular weight polymers ($M_w > 10^4$). At 100 °C, however, the polymerization leveled off in the later stages of the reactions to result in the lower molecular weights, probably because of the side reactions such as the termination between two radicals or the thermal decomposition of the catalyst. When the ratio of ligand to catalyst ($[PMDETA]_0/[CuCl]_0$) was decreased to 2.0, both the polymer yield and the molecular weight decreased (entry 14).

The addition of tin 2-ethylhexanoate [$Sn(EH)_2$] was further investigated for the polymerization of **2** with the $FeCl_2$/P*n*-Bu_3 and CuCl/PMDETA systems for acceleration of the polymerization in which the tin additive might work as a reducing agent for the accumulated oxidized Fe- and Cu-species.[28,29] As also shown in Table 1, $Sn(EH)_2$ increased the polymerization rate as well as the molecular weights in both the Fe- and Cu-catalyzed polyadditions (entry 19 vs 2 for Fe; entry 20 vs 12 for Cu). These suggest that a small amount of the metal catalysts was deactivated during the reactions and that the polymerizations can be enhanced by the addition of some reducing agents. However, the molecular weight distributions became broader than 2 upon the addition of $Sn(EH)_2$, which suggests a deviation from the ideal step-growth polymerization, especially with the CuCl/PMDETA/$Sn(EH)_2$ system. (See also Figure S11 in the Supporting Information.)

Analysis of the Mechanism of Radical Polyaddition Using Model Reactions. To confirm the polymerization mechanism and to clarify possible side reactions, the model reactions for the radical polyaddition were investigated between methyl

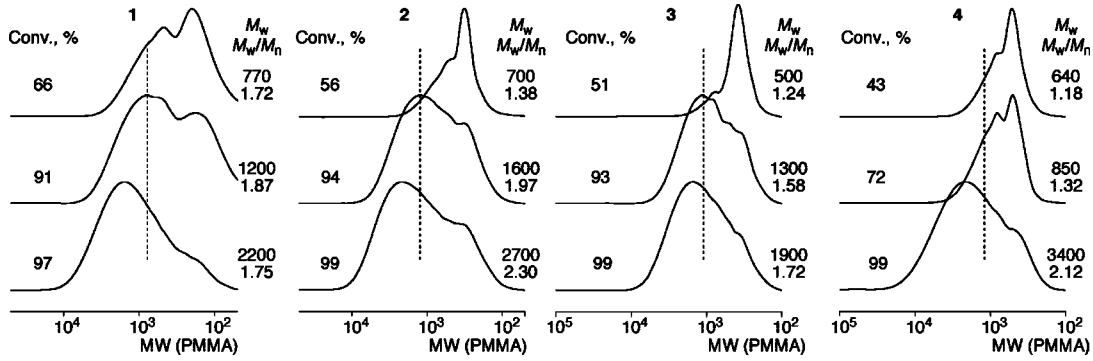

Figure 3. Size exclusion chromatograms of the products in the polyaddition of **1**, **2**, **3**, and **4** (Scheme 1) with $FeCl_2$/tri-*n*-butylphosphine (P*n*-Bu_3): $[monomer]_0 = 2.0$ M; $[FeCl_2]_0 = 100$ mM; $[Pn\text{-}Bu_3]_0 = 200$ mM in toluene at 100 °C.

Table 1. Metal-Catalyzed Radical Polyaddition of 2 (See Scheme 1 for Structure)[a]

entry	metal catalyst	ligand[b]	$[ligand]_0$, mM	$[M]_0$, M	temp, °C	time, h	conv., %[c]	M_w[d]	M_w/M_n[d]
1	$RuCp^*Cl(PPh_3)_2$			2.0	100	530	49	960	1.93
2	$FeCl_2$	P*n*-Bu_3	100	4.0	100	1100	91	1200	1.83
3	$FeCl_2$	P*n*-Bu_3	200	4.0	100	250	91	1200	1.95
4	$FeCl_2$	P*n*-Bu_3	400	4.0	100	300	76	910	1.59
5	$FeCl_2$	P*n*-Bu_3	200	4.0	80	1700	97	1700	1.98
6	$FeCl_2$	P*n*-Bu_3	200	2.0	100	800	99	2700	2.30
7	$FeCl_2$	PCy_3	200	2.0	100	2200	95	1400	1.59
8	$FeCl_2$	PPh_3	200	2.0	100	2200	97	1700	2.05
9	$FeCl_2$	PMDETA	400	4.0	100	240	30	1300	1.85
10	CuCl	PMDETA	400	4.0	100	240	91	3600	3.51
11	CuCl	PMDETA	400	4.0	80	240	97	5500	3.30
12	CuCl	PMDETA	400	4.0	60	1400	99	11 000	4.12
13	CuCl	PMDETA	400	4.0	40	1400	99	9700	2.98
14	CuCl	PMDETA	200	4.0	60	350	58	830	1.66
15	CuCl	PMDETA	400	2.0	60	600	97	5400	2.14
16	CuCl	Me_6TREN	400	2.0	60	1200	90	1500	1.87
17	CuCl	HMTETA	400	2.0	60	1600	88	1800	1.74
18	CuCl	bpy	400	2.0	100	300	39	900	1.74
19[e]	$FeCl_2$	P*n*-Bu_3	200	4.0	100	480	>99	3500	2.32
20[e]	CuCl	PMDETA	400	4.0	60	490	>99	21 000	4.60

[a] $[metal\ catalyst]_0 = 100$ mM, in toluene. [b] Tri-*n*-butylphosphine (P*n*-Bu_3), tricyclohexylphosphine (PCy_3), triphenylphosphine (PPh_3), *N*,*N*,*N*′,*N*″,*N*″-pentamethyldiethylenetriamine (PMDETA), tris[2-(dimethylamino)ethyl]amine (Me_6TREN), 1,1,4,7,10,10-hexamethyltriethylenetetramine (HMTETA), 2,2′-bipyridine (bpy). [c] Determined by gas chromatography. [d] Weight-average molecular weight (M_w) and distribution (M_w/M_n) were determined by SEC. [e] Tin 2-ethylhexanoate [$Sn(EH)_2$] was added ($[Sn(EH)_2]_0 = 45$ mM).

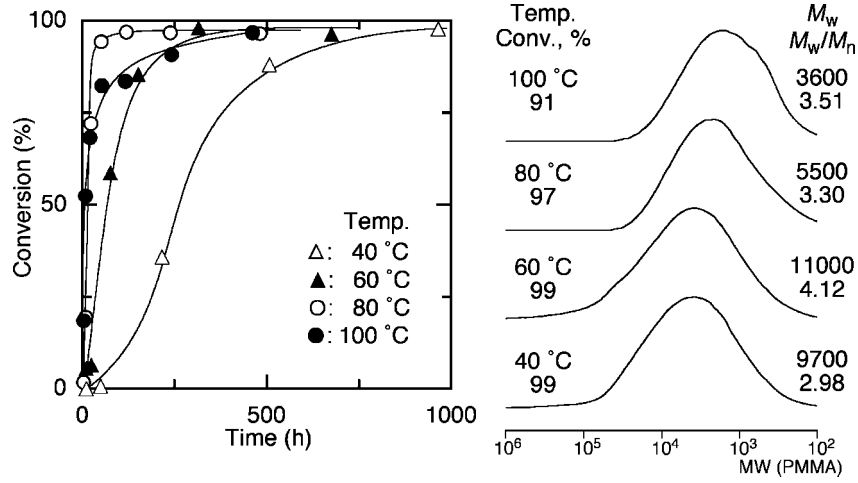

Figure 4. Time−conversion curves and size exclusion chromatograms for the polyaddition of 3-butenyl 2-chloropropionate (**2**) to CuCl/*N*,*N*,*N*′,*N*″,*N*″-pentamethyldiethylenetriamine (PMDETA) at various temperature: $[2]_0 = 4.0$ M; $[CuCl]_0 = 100$ mM; $[PMDETA]_0 = 400$ mM in toluene at (△) 40, (▲) 60, (○) 80, or (●) 100 °C.

2-chloropropionate (**5**) and 3-butenyl acetate (**6**), which correspond to the model C−Cl and C═C parts for **2**, respectively, by using various transition-metal complexes (Scheme 2). Figure 5 shows the consumptions of the chloride (**5**) and vinyl (**6**) compounds with $FeCl_2$/P*n*-Bu_3 at 100 °C and CuCl/PMDETA at 60 °C. In both cases, the two compounds were smoothly and simultaneously consumed at the same rate to nearly quantitative conversions (>90%) to produce the 1:1 adduct (**7**) almost quantitatively, as shown later. In the later stages of the reactions, however, the consumptions of C−Cl (**5**) became slightly faster than those of C═C (**6**), suggesting the existence of a small amount of side reactions.

Scheme 2. Atom Transfer Radical Addition of Model Compounds

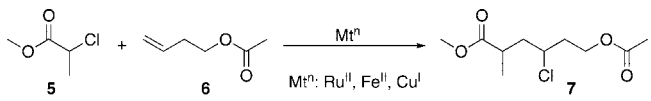

Table 2. Model Reactions between Methyl 2-Chloropropionate (5) and 3-Butenyl Acetate (6) with Various Metal Catalysts[a]

			conv., %[c]				
entry	catalyst/ligand[b]	time, h	**5**	**6**	**7**, %[d]	**8**, %[e]	**9**, %[f]
1	$RuCp^*Cl(PPh_3)_2$	35	42	43	28 (66)	4 (13)	n.d.[g]
2	$RuCp^*Cl(PPh_3)_2$	150	63	46	37 (81)	3 (8)	<1
3	$FeCl_2$/P*n*-Bu_3	10	52	51	50 (98)	1 (2)	n.d.[g]
4	$FeCl_2$/P*n*-Bu_3	70	88	86	87 (>99)	2 (2)	<1
5	$FeCl_2$/PMDETA	35	39	0	0 (0)	3	n.d.[g]
6	$FeCl_2$/PMDETA	200	57	6	2 (36)	<1	n.d.[g]
7	CuCl/PMDETA	110	62	59	59 (>99)	n.d.	n.d.[g]
8	CuCl/PMDETA	240	80	74	73 (99)	2 (3)	n.d.[g]
9	CuCl/PMDETA	600	95	84	84 (>99)	5 (6)	n.d.[g]

[a] $[\mathbf{5}]_0 = 2.0$ M; $[\mathbf{6}]_0 = 2.0$ M. [b] [metal catalyst]$_0 = 100$ mM; $[P\textit{n}\text{-}Bu_3]_0 = 200$ mM; $[PMDETA]_0 = 400$ mM; in toluene at 100 °C (for Ru and Fe) or 60 °C (for Cu); tri-*n*-butylphosphine (P*n*-Bu_3), *N*,*N*′,*N*″,*N*‴,*N*‴′-pentamethyldiethylenetriamine (PMDETA). [c] Determined by gas chromatography. [d] 1:1 adduct (**7**, see Scheme 2 for structure) yield was determined by ^{1}H NMR. The values in parentheses indicate the yields based on the consumptions of **6**. [e] Content of methyl propionate (**8**) was determined by gas chromatography. The values in parentheses indicate the relative ratio to **7**. [f] Content of dimethyl 2,3-dimethylsuccinate (**9**) was determined by gas chromatography. [g] Not being detected.

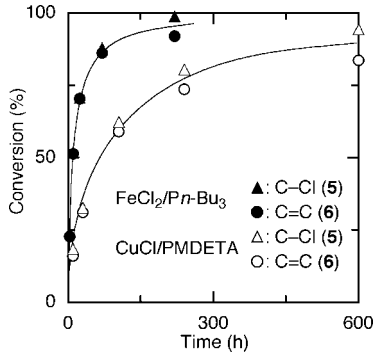

Figure 5. Time−conversion curves for the model Kharasch reactions between methyl 2-chloropropionate (**5**) and 3-butenyl acetate (**6**) with $FeCl_2$/tri-*n*-butylphosphine (P*n*-Bu_3) (▲, ●, respectively) or CuCl/*N*,*N*,*N*′,*N*″,*N*‴-pentamethyldiethylenetriamine (PMDETA) (△, ○, respectively): $[\mathbf{5}]_0 = [\mathbf{6}]_0 = 2.0$ M; $[MtX_n]_0 = 100$ mM; $[P\textit{n}\text{-}Bu_3]_0 = 200$ mM; $[PMDETA]_0 = 400$ mM in toluene at 100 (for $FeCl_2$/P*n*-Bu_3) or 60 °C (for CuCl/PMDETA).

Various metal complexes were also employed in the model reactions. Table 2 summarizes the conversions of **5** and **6** and the yields of the adduct (**7**) along with the contents of byproducts, methyl propionate (**8**) and dimethyl 2,3-dimethylsuccinate (**9**). The latter compound would be generated via the combination of the radical species derived from **5**, whereas the former compound would be generated via disproportionation or hydrogen transfer from other compounds or solvents. Among them, the $FeCl_2$/P*n*-Bu_3 (entries 3 and 4) and CuCl/PMDETA (entries 7−9) systems induced the simultaneous consumptions of **5** and **6** at almost the same rate and gave the corresponding 1:1 adduct in good yield. Furthermore, the conversions of **6** were almost the same with the yields of the 1:1 adduct, indicating that no consecutive vinyl additions of **6** to the radical species took place. This also supports the fact that the $FeCl_2$/P*n*-Bu_3 and CuCl/PMDETA systems polymerized **2** exclusively via polyaddition mechanism not via consecutive vinyl-addition chain-growth polymerization. The detailed analysis of the byproducts in the model reactions also gave useful information

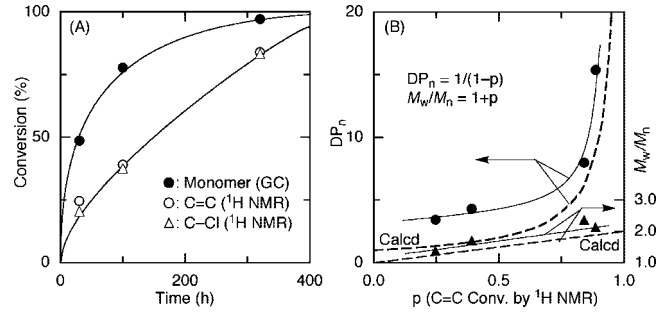

Figure 6. (A) Time−conversion curves and (B) number-average polymerization degree (DP_n) and molecular weight distribution (M_w/M_n) as a function of C=C conversion for the polyaddition of 3-butenyl 2-chloropropionate (**2**) to CuCl/*N*,*N*′,*N*″,*N*‴,*N*‴′-pentamethyldiethylenetriamine (PMDETA): $[\mathbf{2}]_0 = 2.0$ M; $[CuCl]_0 = 100$ mM; $[PMDETA]_0 = 400$ mM in toluene at 60 °C.

for understanding the polymerization. The negligible amount of combination products (**9**) means almost no significant coupling reactions between **2** and the oligomers/polymers, which might have led to a molecular weight increase via the polymer−polymer coupling as well as the formation of the polymers with vinyl groups at both ends. However, a minimal formation (<2%) of **8** suggests a slight loss of the halogens at the polymer terminals, which would prevent the molecular weight increase, especially in the later stages of the polymerization.

With the other metal catalyst systems, such as $RuCp^*(PPh_3)_2$ (entries 1 and 2) and $FeCl_2$/PMDETA (entries 5 and 6), one of the components was consumed much faster than the other to result in a lower yield of the adduct and a higher content of the byproducts. These results indicate that one of the best catalytic systems for the model radical addition reaction is the $FeCl_2$/P*n*-Bu_3 or CuCl/PMDETA system, which is also the best catalytic system for the radical polyaddition, as shown above. Therefore, the search for a good catalyst for the corresponding model radical addition is helpful for the design of a good catalyst for the radical polyaddition.

We investigated a more detailed mechanism of the radical polyaddition by measuring the total consumptions of the C=C and C−Cl groups that originated from **2** and the polymerized products by ^{1}H NMR, whereas the consumption of monomer **2** was measured by gas chromatography. As shown in Figure 6A, the consumptions of the C=C and C−Cl groups simultaneously occurred at the same rate, indicating the 1:1 reaction. The rates were close to those for the model reactions (Figure 5), suggesting the polyaddition via a similar radical addition reaction. Furthermore, the conversions of the functional groups (C=C and C−Cl) were consistently lower than those of the monomer. In particular, those of the functional groups (C=C and C−Cl) for the 49% monomer conversion were ∼25%, almost half of the monomer conversion. These results indicate that most of the consumed monomers were converted to dimers without any significant intramolecular cyclization in the initial stages; then the reaction between the oligomers proceeded via an intermolecular polyaddition to result in the polymers.

As shown in Figure 6B, the number-average polymerization degree (DP_n) of the products progressively increased and was close to the calculated line for the step-growth polymerization based on the assumption that the DP_n increases in inverse proportion to 1−p, where p means the consumption of the functional group or the extent of reaction. In addition, the molecular weight distribution increased with the conversion and was close to the calculated value of 2 ($M_w/M_n \approx 2$). All of these relationships are typical for a step-growth polymerization and thus indicate that the polymers were produced via the expected intermolecular polyaddition on the basis of the metal-catalyzed

C−Cl activation, followed by the radical addition to C═C.

Therefore, the polymerization with the optimized systems most probably proceeds via step-growth mechanism of successive ATRA without the chain-growth reaction of the vinyl groups, because both C−Cl and C═C bonds are consumed at the same rate (see also Figure 6). However, similar to the metal-catalyzed living polymerizations, the radical species derived from the C−Cl bond suffers from minimal side reactions. A loss of the halogens at the polymer terminals would set a limit on the molecular weights and would decrease the reaction rate and the final conversion of the monomers because of the accumulation of the higher oxidation state metal species. However, we have recently found that iron(III) chloride ($FeCl_3$) can become active in the presence of P*n*-Bu_3 without any added reducing agents to induce living radical polymerizations,[30] which may also support the highly effective $FeCl_2$/P*n*-Bu_3 system in the polyaddition reactions. Therefore, the conditions, such as the choice of both metal and ligand, concentrations of monomer and catalyst, and reaction temperature, are essential to the effective radical polyadditions by minimizing the side reactions such as vinyl chain-growth polymerization, radical termination, and intramolecular cyclization.

A further mechanism study was done by NMR analysis of the products obtained from the radical polyaddition of **2** and the model radical addition between **5** and **6**. Figure 7 shows the ^{1}H−^{1}H COSY NMR spectra of the model adduct (**7**) prepared from **5** and **6** and the polymer of **2** obtained by the CuCl/PMDETA system. In both 1D spectra, similar main peaks (*a*′−*f*′ and *a*−*f*) were observed. A series of similar cross-peaks (*b*−*a*, *b*−*c*, *d*−*c*, *d*−*e*, *f*−*e*) were also observed in both of the 2D spectra. The peaks *a*−*f* can thus be assigned to the main chain protons of the aliphatic polyester with the C−Cl pendants. In addition to these main peaks, the polymer spectra exhibited small sharp peaks that originated from the protons neighboring vinyl (1 and 2) and chlorine (3 and 4) groups at the α and *ω* ends, respectively. The DP_n of the polymers can be determined from the peak intensity ratio (*b*/1) of the methylene protons (1) adjacent to the terminal vinyl group to the methine (*b*) in the main chain unit of the polyester. The M_n(NMR) calculated from the DP_n and the formula weight of **2** was 850, which was lower than the molecular weight determined by SEC [M_n(SEC) = 1400], which was most probably due to the SEC standards of poly(methyl methacrylate). These NMR studies also support the fact that the metal-catalyzed radical polyaddition reactions mainly proceed via formation of the C−C linkage and the inactive C−Cl pendant to result in the polyester main chain predominantly with no visible formation of consecutive chain-growth vinyl-addition structures under the optimized conditions.

The thermal properties of the polyesters obtained from the metal-catalyzed polyaddition of **1** and **2** were also evaluated by differential scanning calorimetry (DSC) (Table 3 and Figure S12 in the Supporting Information). The glass-transition temperatures (T_g) were observed for all of the polymers, which depended on the molecular weights of the polymers similar to general polymers. The DSC curves of the obtained polyesters with higher molecular weights exhibited endothermal peaks because of the melting temperatures (T_m). This indicates that the well-defined polyesters prepared by the metal-catalyzed radical polyaddition exhibited a crystalline domain like the usual aliphatic polyesters, whereas a similar brominated aliphatic polyester prepared by ring-opening polymerization was amorphous and showed no tendency to be crystalline, even with a high molecular weight.[31]

Combination with Metal-Catalyzed Living Radical Polymerization for Block Copolymerization. The polymers obtained by the metal-catalyzed radical polyaddition have a C−Cl bond at the *ω* terminal, which can work as an initiating site for the living radical addition polymerization of vinyl monomers to form the block copolymers consisting of the polyesters and the vinyl polymers. The polyester of **2** bearing

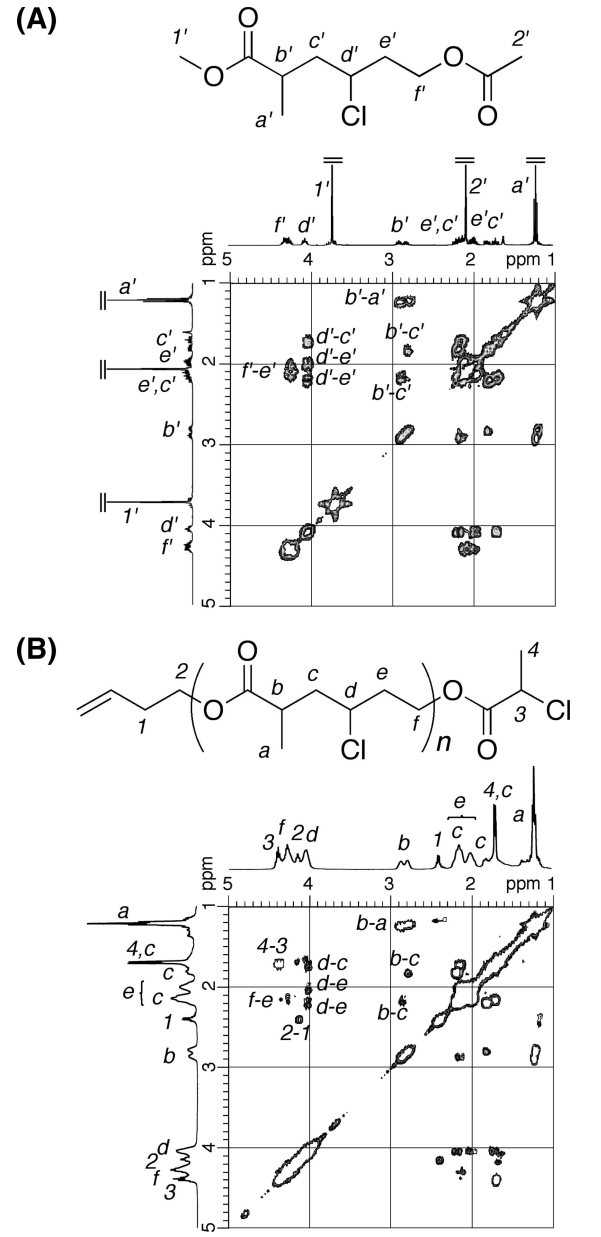

Figure 7. ^{1}H−^{1}H correlation spectra of (A) the adduct (**7**) prepared from (A) methyl 2-chloropropionate (**5**) and 3-butenyl acetate (**6**) and (B) the polymer of 3-butenyl 2-chloropropionate (**2**) obtained with CuCl/*N*,*N*,*N*′,*N*″,*N*″-pentamethyldiethylenetriamine (PMDETA) in toluene at 60 °C ($CDCl_3$, r.t.).

Table 3. Thermal Analysis of Polyesters Obtained by Radical Polyaddition

entry	polymer	T_g, °C[d]	T_m, °C[d]	M_n(SEC)[e]	M_n(NMR)[f]
1	poly(**1**)[a]	−13.8		1700	1800
2	poly(**2**)[b]	−24.9		1600	2300
3	poly(**2**)[a]	8.5	151.9	5000	4100
4	poly(**2**)[c]	8.7	152.2	4800	3400

[a] Obtained with CuCl/*N*,*N*,*N*′,*N*″,*N*″-pentamethyldiethylenetriamine (PMDETA) in toluene at 60 °C; See Scheme 1 for structures. [b] Obtained with $FeCl_2$/tri-*n*-butylphosphine/tin 2-ethylhexanoate in toluene at 100 °C; See Scheme 1 for structures. [c] Obtained with CuCl/PMDETA/tin 2-ethylhexanoate in toluene at 60 °C. [d] Glass-transition temperature (T_g) and melting temperature (T_m) were determined by DSC. [e] Number-average molecular weight (M_n) determined by SEC. [f] M_n determined from the α-end functionalities by ^{1}H NMR; See Figure 7.

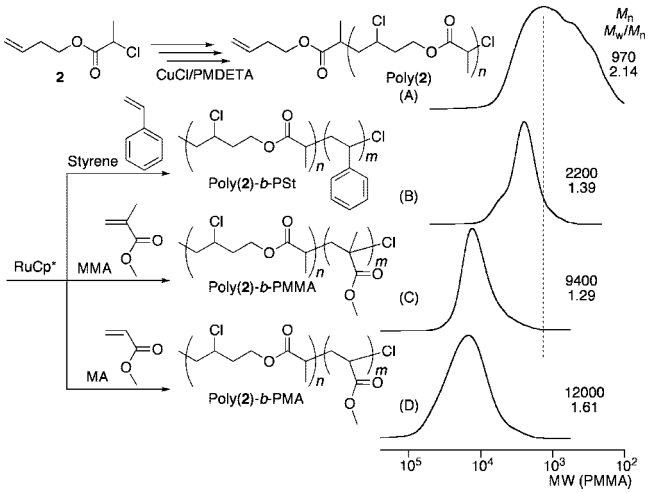

Figure 8. Size exclusion chromatograms of the polymer of (A) 3-butenyl 2-chloropropionate (**2**), (B) poly(**2**)-*b*-polystyrene, (C) poly(**2**)-*b*-poly(methyl methacrylate), and (D) poly(**2**)-*b*-poly(methyl acrylate) copolymers obtained in the block copolymerization from the macroinitiator poly(**2**) with RuCp*Cl(PPh_3)$_2$: [styrene, methyl methacrylate, or methyl acrylate]$_0$ = 4.0 M, [poly(**2**)]$_0$ = 10 mM, [RuCp*Cl(PPh_3)$_2$]$_0$ = 4 mM, [tri-*n*-butylamine]$_0$ = 40 mM in toluene at 80 °C. Monomer conversion: (B) 5% for styrene; (C) 7% for methyl methacrylate; (D) 20% for methyl acrylate.

an active C−Cl terminal obtained by the CuCl/PMDETA system was then employed as a macroinitiator in the ruthenium-catalyzed living radical polymerization of various vinyl monomers. The block copolymerizations of styrene, MMA, and MA from the macroinitiator were carried out with RuCp*Cl(PPh_3)$_2$ in toluene at 80 °C in the presence of tri-*n*-butylamine (*n*-Bu_3N) as an additive (Figure 9).[24,32] All of the vinyl monomers were smoothly consumed to result in a higher molecular weight shift of the SEC curves while maintaining unimodal MWDs, which became narrower (M_w/M_n = 1.3 to 1.6) than the starting polyester. This suggests the formation of the block copolymers of **2** and the vinyl monomers. However, with consumption of the vinyl monomers, the MWDs became broader and bimodal because of the intermolecular addition of a growing radical block polymer chain end to the C═C double-bond terminal of another block polymer chain.

The structures of the obtained block copolymers were then analyzed by ^{1}H NMR. Figure 9 shows the ^{1}H NMR spectra of poly(**2**) and poly(**2**)-*b*-poly(MA) at 20% MA conversion, which were purified by a chromatographic column packed with silica gel and preparative SEC to remove the residual monomer and catalyst for poly(**2**) and the block copolymer, respectively. The spectrum of the block copolymer exhibited typical changes in which the signal of the methine proton (5) adjacent to the reactive chloride terminal in poly(**2**) completely disappeared, whereas the other peaks (*a*−*f*, 1−4) were intact. In addition, large broad peaks (*g*−*i*), assignable to the protons of the repeating units in the poly(MA) part, appeared. The methoxy proton (*i*′) at the *ω* terminal of the MA unit, which is adjacent to the chlorine, also appeared at 3.8 ppm. The DP$_n$ of **2** and the MA units in the block copolymers can be determined from the peak intensity ratios (3*e*/*i*′ and *i*/*i*′) of the methyl protons (*i*′) adjacent to the terminal chlorine group to the methine protons (*e*) of the polyester unit and the methyl protons (*i*) of the poly(MA) unit, respectively [DP$_n$(**2**) = 6.4; DP$_n$(MA) = 163]. The M_n(NMR, *ω* end) calculated from each DP$_n$ was 15 100, which was close to the molecular weight determined by SEC [M_n(SEC) = 14 800]. These results also indicate that the block copolymerization successfully proceeded using the polyester obtained from the metal-catalyzed polyaddition as a macroinitiator in conjunction with the metal-catalyzed living radical polymerization of vinyl monomers.

Conclusions

The metal-catalyzed ATRA was successfully converted into the metal-catalyzed radical polyaddition using the ester-linked monomers, which bear both a C−Cl bond and a C═C double bond in a single molecule, to produce the polyesters under various conditions via a step-growth mechanism. The obtained polyester had a precisely controlled structure of repeating main-chain ester units with the unreactive C−Cl pendants in addition to a reactive C−Cl and unconjugated C═C double bond terminals. The terminal chlorine can also be activated again by the metal catalyst to initiate the living radical polymerization of the vinyl monomers forming novel block copolymers consisting of polyesters and vinyl polymers. We believe that this radical polyaddition will provide new strategies in not only exploring novel polymerization mechanisms but also designing novel polymer structures.

Experimental Section

Materials. MMA (TCI, >98%), MA (Tokyo Kase, >99%), styrene (Wako Chemicals, >98%), allyl acetate (Aldrich, 99%) and methyl 2-chloropropionate (TCI, >95%) were distilled from calcium hydride under reduced pressure before use. $RuCl_2(PPh_3)_3$ (Aldrich, 97%), $FeCl_2$ (Aldrich, 99.99%), CuCl (Aldrich, 99.99%), and RuCp*Cl(PPh_3)$_2$ (provided from Wako Chemicals) were used as received. All metal compounds were handled in a glovebox (VAC Nexus) under a moisture- and oxygen-free argon atmosphere (O_2, < 1 ppm). Toluene was distilled over sodium benzophenone ketyl and bubbled with dry nitrogen for 15 min just before use. P*n*-Bu_3 (KANTO, >98%), PCy_3 (KANTO, >97%), PPh_3 (KANTO, >98%), bpy (Kishida, >99%), and Sn(EH)$_2$ (Aldrich, ∼95%) were used as received. *n*-Bu_3N, PMDETA, Me_6TREN, HMTETA, and 3-butenyl acetate were distilled from calcium hydride before use.

Monomer Synthesis (1−4). Allyl 2-chloropropionate (**1**), 3-butenyl 2-chloropropionate (**2**), 4-pentenyl 2-chloropropionate (**3**), and 2-(allyloxy)ethyl 2-chloropropionate (**4**) were synthesized from 2-chloropropionyl chloride (TCI, >95%) and the corresponding alcohols, that is, allyl alcohol (KANTO, >99%), 3-buten-1-ol (TCI, >98%), 4-penten-1-ol (TCI, >98%), and 2-allyloxyethanol (TCI, >98%) for **1**−**4**, respectively. The reaction was carried out by the use of a syringe technique under a dry argon atmosphere in an oven-dried glass tube equipped with three-way stopcocks. A typical synthetic example for **2** is given below. 2-Chloropropionyl chloride (51.0 mL, 0.525 mol) was added dropwise with vigorous stirring to a solution of 3-buten-1-ol (42.4 mL, 0.500 mol) and triethylamine (76.7 mL, 0.550 mol) in dry THF (79.9 mL) at 0 °C. The mixture was stirred for 1 h at 0 °C and then for 12 h at room temperature. After the dilution with diethyl ether, the mixture was washed with the aqueous solution of $NaHCO_3$ and then NaCl and was evaporated to remove the solvents. The monomer was distilled over calcium hydride under reduced pressure to give pure 3-butenyl 2-chloropropionate (**2**) (56.0 mL, 0.354 mol; yield = 70.9%, purity >99%). (See Figure 1 for the ^{1}H NMR spectra of the monomers (**1**−**4**).) Monomer (**1**): ^{1}H NMR ($CDCl_3$, *δ*): 1.70−1.72 (d, 3H, CH−CH_3, *J* = 7.0 Hz), 4.40−4.46 (q, 1H, C*H*−CH$_3$, *J* = 7.0 Hz), 4.66−4.69 (dq, 2H, CH_2OCO, *J* = 5.7, 1.2 Hz), 5.27−5.40 (dq, dq, 2H, CH_2=CH, *J* = 10.4, 1.3 Hz, *J* = 17.2, 1.5 Hz), 5.88−5.98 (ddt, 1H, CH$_2$=C*H*, *J* = 17.2, 10.4, 5.7 Hz). Monomer (**2**): ^{1}H NMR ($CDCl_3$, *δ*): 1.68−1.69 (d, 3H, CH−CH_3, *J* = 7.0 Hz), 2.40−2.46 (qt, 2H, CH$_2$=CH−CH_2, *J* = 6.7, 1.3 Hz), 4.22−4.25 (t, 2H, CH_2OCO, *J* = 6.8 Hz), 4.37−4.42 (q, 1H, C*H*−CH$_3$, *J* = 6.9 Hz), 5.08−5.16 (dq, dq, 2H, CH_2=CH, *J* = 10.3 Hz, 1.3 Hz, *J* = 17.4, 1.7 Hz), 5.73−5.84 (ddt, 1H, CH$_2$=C*H*, *J* = 17.2, 10.3, 6.8 Hz). Monomer (**3**): ^{1}H NMR ($CDCl_3$, *δ*): 1.68−1.70 (d, 3H, CH−CH_3, *J* = 6.9 Hz), 1.75−1.82 (m, 2H, CH_2−CH$_2$OCO), 2.12−2.18 (m, 2H, CH$_2$=CH−CH_2), 4.17−4.21 (td, 2H, CH_2OCO, *J* = 6.6, 2.6 Hz), 4.37−4.42 (q, 1H, C*H*−CH$_3$, *J* = 6.9 Hz), 4.99−5.08 (ddt,

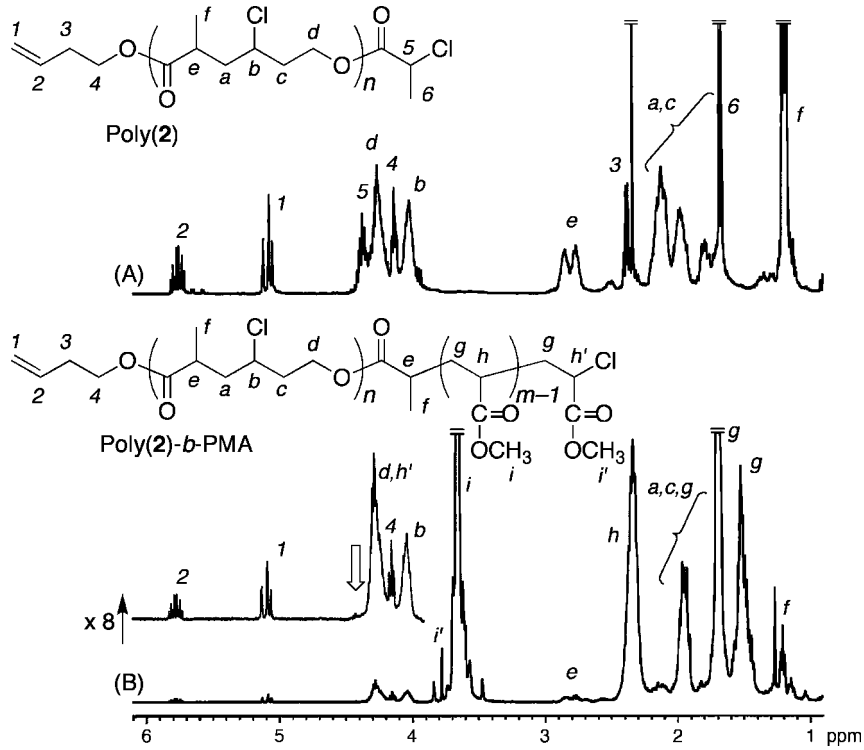

Figure 9. ^{1}H NMR spectra of (A) the polymer of 3-butenyl 2-chloropropionate (**2**) (number-average molecular weight (M_n) = 970, molecular weight distribution (M_w/M_n) = 2.14) and (B) poly(**2**)-*b*-poly(methyl acrylate) (M_n =14 800, M_w/M_n = 1.45) obtained in the same experiment as that for Figure 8 ($CDCl_3$, 55 °C).

dq, 2H, C*H*$_2$=CH, *J* = 10.2, 1.9, 1.2 Hz, *J* = 17.0, 1.7 Hz), 5.75−5.85 (dt, 1H, CH$_2$=C*H*, *J* = 17.0, 10.3, 6.6 Hz). Monomer (**4**): ^{1}H NMR ($CDCl_3$, δ): 1.70−1.71 (d, 3H, CH−C*H*$_3$, *J* = 7.0 Hz), 3.67−3.69 (m, 2H, C*H*$_2$−CH$_2$OCO), 4.02−4.05 (dt, 2H, CH$_2$=CH−C*H*$_2$, *J* = 5.7, 1.3 Hz), 4.33−4.35 (m, 2H, C*H*$_2$OCO), 4.41−4.46 (q, 1H, C*H*−CH$_3$, *J* = 6.9 Hz), 5.19−5.32 (dq, dq, 2H, C*H*$_2$=CH, *J* = 10.3, 1.4 Hz, *J* = 17.2, 1.6 Hz), 5.85−5.95 (ddt, 1H, CH$_2$=C*H*, *J* = 17.2, 10.4, 5.7 Hz).

Polymerization. Polymerization was carried out under dry nitrogen in baked glass tubes equipped with a three-way stopcock. Typically, a mixture of $FeCl_2$ (50.7 mg, 0.40 mmol) and P*n*-Bu_3 (0.20 mL, 0.80 mmol) in toluene (2.54 mL) was stirred for 24 h at 80 °C to give a homogeneous solution of $FeCl_2$(P*n*-Bu_3)$_2$ complex. After the solution was cooled to room temperature, 3-butenyl 2-chloropropionate (**2**) (1.26 mL, 8.0 mmol) was added. The solution was evenly charged in seven glass tubes, and the tubes were sealed by flame under a nitrogen atmosphere. The tubes were immersed in a thermostatic oil bath at 100 °C. In predetermined intervals, the polymerization was terminated by cooling the reaction mixtures to −78 °C. Monomer conversion was determined from the concentration of residual monomer measured by gas chromatography with toluene as an internal standard (800 h, 99% conversion). The quenched reaction mixture was diluted with ethyl acetate (30 mL), washed with dilute citric acid and water to remove complex residues, evaporated to dryness under reduced pressure, and vacuum dried to give the product polymers (0.14 g, 87% yield; M_n = 1200, M_w = 2700, M_w/M_n = 2.30), including a small amount of remaining catalyst residues.

Model Radical Addition. Radical addition reaction was carried out under dry nitrogen in baked glass tubes equipped with a three-way stopcock. Typically, a mixture of $FeCl_2$ (50.7 mg, 0.40 mmol) and P*n*-Bu_3 (0.20 mL, 0.80 mmol) in toluene (1.88 mL) was stirred for 24 h at 80 °C to give a homogeneous solution of $FeCl_2$(P*n*-Bu_3)$_2$ complex. After the solution was cooled to room temperature, methyl 2-chloropropionate (**5**) (0.91 mL, 8.0 mmol) and 3-butenyl acetate (**6**) (1.01 mL, 8.0 mmol) were added. The solution was evenly charged in seven glass tubes, and the tubes were sealed by flame under a nitrogen atmosphere. The tubes were immersed in a thermostatic oil bath at 100 °C. In predetermined intervals, the reaction was terminated by cooling the reaction mixtures to −78 °C. The conversions of the functional groups (C=C and C−Cl) and the yields of the adducts were determined from the concentration of **5**, **6**, and **7** measured by ^{1}H NMR spectroscopy with toluene as an internal standard (88 and 86% conversions and 87% yield, respectively, in 70 h). The contents of the byproducts, methyl propionate (**8**) and dimethyl 2,3-dimethylsuccinate (**9**), were measured by gas chromatography with methyl 2-chloropropionate as an internal standard (2 and <1%, respectively, in 70 h). The quenched reaction mixture was diluted with toluene (30 mL), washed with dilute citric acid and water to remove complex residues, evaporated to dryness under reduced pressure, and vacuum dried. The residue was purified by column chromatography and eluted with diethyl ether to give the 1:1 adduct (**7**) as a mixture of diastereomers because of two asymmetric carbons, that is, two pairs of enantiomers: (2*R*,4*R*)- and (2*S*,4*S*)- or (2*R*,4*S*)- and (2*S*,4*R*)-isomers (ratio of diastereomers = 51:49). Yield: 0.16 g (68%). ^{1}H NMR ($CDCl_3$, δ): 1.21 (dd, 3H, CH−C*H*$_3$), 1.67−1.75, 1.76−1.85, 2.08−2.22 (m, 2H, CH−C*H*$_2$−CHCl), 1.93−2.04, 2.08−2.22 (m, 2H, CHCl−C*H*$_2$−CH$_2$O), 2.06 (d, 3H, OCOC*H*$_3$), 2.75−2.92 (m, 1H, OCOC*H*), 3.70 (d, 3H, C*H*$_3$OCO), 3.99−4.07 (m, 1H, C*H*Cl), 4.15−4.32 (m, 2H, C*H*$_2$OCO). ^{13}C NMR ($CDCl_3$, δ): 16.23, 18.28 (CH−*C*H$_3$), 20.97, 20.99 (OCO*C*H$_3$), 36.71, 36.78 (OCO*C*H), 37.43, 37.69 (CHCl−*C*H$_2$−CH$_2$O), 41.58, 42.45 (CH−mdit > CH$_2$−CHCl), 51.78, 51.84 (*C*H$_3$OCO), 57.16, 58.15 (*C*HCl), 61.26, 61.29 (*C*H$_2$OCO), 170.66, 170.69 (O*C*OCH$_3$), 176.06, 176.15 (CH$_3$O*C*O).

Measurements. Monomer conversion was determined from the concentration of residual monomer measured by gas chromatography (Shimadzu GC-8A equipped with a thermal conductivity detector and a 3.0 mm i.d. × 2 m stainless-steel column packed with SBS-200 (Shinwa Chemical Industries) supported on Shimalite W; injection and detector temperature = 200 °C, column temperature = 160 °C) with toluene as an internal standard under He gas flow. ^{1}H NMR and COSY spectra were recorded in $CDCl_3$ at room temperature on a Varian Gemini 2000 spectrometer operating at 400 MHz. The number-average molecular weight (M_n), the weight-average molecular weight (M_w), and the molecular weight distribution (M_w/M_n) of the product polymers were determined by SEC in

THF at 40 °C on two polystyrene gel columns (Shodex K-805 L (pore size: 20−1000 Å; 8.0 mm i.d. × 30 cm); flow rate 1.0 mL/min) connected to a Jasco PU-980 precision pump and a Jasco 930-RI refractive index detector. The columns were calibrated against eight standard poly(MMA) samples (Shodex; $M_p = 202-1\,950\,000$; $M_w/M_n = 1.02$ to 1.09). The glass-transition temperature (T_g: midpoint of the transition) and melting temperature (T_m: endothermic maximum) of the polymers were recorded on SSC-5200 DSC (Seiko Instruments). Certified indium and tin were used for temperature and heat flow calibration. Samples were first heated to 100 or 150 °C at 10 °C/min, equilibrated at this temperature for 0 or 10 min, and cooled to −100 at 10 °C/min. After being held at this temperature for 20 min, the samples were then reheated to 200 °C at 10 °C/min. All T_g and T_m values were obtained from the second scan after the thermal history was removed.

Acknowledgment. This work was partially supported by a Grant-in-Aid for Young Scientists (S) (no. 19675003) by the Japan Society for the Promotion of Science and the Global COE Program "Elucidation and Design of Materials and Molecular Functions."

Supporting Information Available: ^{1}H NMR spectra of poly(**1**−**4**), SEC curves of monomers (**1** and **2**) and their oligomers, DSC of poly(**2**), and time−conversion, conversion−M_w, and SEC curves for polyaddition. This material is available free of charge via the Internet at http://pubs.acs.org.

References and Notes

(1) (a) Kharasch, M. S.; Jensen, E. V.; Urry, W. H. *Science* **1945**, *102*, 128. (b) Minisci, F. *Acc. Chem. Res.* **1975**, *8*, 165–171. (c) Iqbal, J.; Bhatia, B.; Nayyar, N. K. *Chem. Rev.* **1994**, *94*, 519–564. (d) Gossage, R. A.; van de Kuil, L. A.; van Koten, G. *Acc. Chem. Res.* **1998**, *31*, 423–431.

(2) (a) Kato, M.; Kamigaito, M.; Sawamoto, M.; Higashimura, T. *Macromolecules* **1995**, *28*, 1721–1723. (b) Kamigaito, M.; Ando, T.; Sawamoto, M. *Chem. Rev.* **2001**, *101*, 3689–3745. (c) Kamigaito, M.; Ando, T.; Sawamoto, M. *Chem. Rec.* **2004**, *4*, 159–175.

(3) (a) Wang, J.-S.; Matyjaszewski, K. *J. Am. Chem. Soc.* **1995**, *117*, 5614–5615. (b) Matyjaszewski, K.; Xia, J. *Chem. Rev.* **2001**, *101*, 2921–2990. (c) Tsarevsky, N. V.; Matyjaszewski, K. *Chem. Rev.* **2007**, *107*, 2270–2299.

(4) Percec, V.; Barboiu, B. *Macromolecules* **1995**, *28*, 7970–7972.

(5) Granel, C.; Dubois, Ph.; Jérôme, R.; Teyssié, Ph. *Macromolecules* **1996**, *29*, 8576–8582.

(6) Haddleton, D. M.; Jasieczek, C. B.; Hannon, M. J.; Shooter, A. J. *Macromolecules* **1997**, *30*, 2190–2193.

(7) Baek, K.-Y.; Kamigaito, M.; Sawamoto, M. *J. Polym. Sci., Part A: Polym. Chem.* **2002**, *40*, 1937–1944.

(8) (a) Ando, T.; Kamigaito, M.; Sawamoto, M. *Macromolecules* **1998**, *31*, 6708–6711. (b) Bon, S. A. F.; Steward, A. G.; Haddleton, D. M. *J. Polym. Sci., Part A: Polym. Chem* **2000**, *38*, 2678–2686.

(9) (a) Coessens, V.; Matyjaszewski, K. *Macromol. Rapid Commun.* **1999**, *20*, 127–134. (b) Coessens, V.; Pyun, J.; Miller, P. J.; Gaynor, S. G.; Matyjaszewski, K. *Macromol. Rapid Commun.* **2000**, *21*, 103–109. (c) Coessens, V.; Pintauer, T.; Matyjaszewski, K. *Prog. Polym. Sci.* **2001**, *26*, 337–377. (d) Müller, A. H. E. *Macromol. Rapid Commun.* **2005**, *26*, 1893–1894.

(10) (a) Paik, H. J.; Gaynor, S. G.; Matyjaszewski, K. *Macromol. Rapid Commun.* **1998**, *19*, 47–52. (b) Matyjaszewski, K.; Teodorescu, M.; Miller, P. J.; Peterson, M. L. *J. Polym. Sci., Part A: Polym. Chem.* **2000**, *38*, 2440–2448.

(11) (a) Gaynor, S. G.; Edelman, S.; Matyjaszewski, K. *Macromolecules* **1996**, *29*, 1079–1081. (b) Matyjaszewski, K.; Gaynor, S. G.; Kulfan, A.; Podwika, M. *Macromolecules* **1997**, *30*, 5192–5194. (c) Matyjaszewski, K.; Gaynor, S. G.; Müller, A. H. E. *Macromolecules* **1997**, *30*, 7034–7041. (d) Matyjaszewski, K.; Gaynor, S. G. *Macromolecules* **1997**, *30*, 7042–7049. (e) Matyjaszewski, K.; Pyun, J.; Gaynor, S. G. *Macromol. Rapid Commun.* **1998**, *19*, 665–670.

(12) Weimer, M. W.; Fréchet, J. M. J.; Gitsov, I. *J. Polym. Sci., Part A: Polym. Chem.* **1998**, *36*, 955–970.

(13) (a) Mori, H.; Böker, A.; Krausch, G.; Müller, A. H. E. *Macromolecules* **2001**, *34*, 6871–6882. (b) Hong, C.-Y.; Pan, C.-Y. *Polymer* **2001**, *42*, 9385–9391. (c) Bibiao, J.; Yang, Y.; Jian, D.; Shiyang, F.; Rongqi, Z.; Jianjun, H.; Wenyun, W. *J. Appl. Polym. Sci.* **2002**, *83*, 2114–2123. (d) Mori, H.; Seng, D. C.; Zhang, M.; Müller, A. H. E. *Langmuir* **2002**, *18*, 3682–3693. (e) Powell, K. T.; Cheng, C.; Wooley, K. L. *Macromolecules* **2007**, *40*, 4509–4515.

(14) (a) Matyjaszewski, K.; Ziegler, M. J.; Arehart, S. V.; Greszta, D.; Pakula, T. *J. Phys. Org. Chem.* **2000**, *13*, 775–786. (b) Borner, H. G.; Duran, D.; Matyjaszewski, K.; da Silva, M.; Sheiko, S. S. *Macromolecules* **2002**, *35*, 3387–3394.

(15) Miura, Y.; Shibata, T.; Satoh, K.; Kamigaito, M.; Okamoto, Y. *J. Am. Chem. Soc.* **2006**, *128*, 16026–16027.

(16) Percec, V.; Barboiu, B.; Grigoras, C.; Bera, T. K. *J. Am. Chem. Soc.* **2003**, *125*, 6503–6516.

(17) (a) Miura, Y.; Kaneko, T.; Satoh, K.; Kamigaito, M.; Jinnai, H; Okamoto, Y *Chem. Asian J.* **2007**, *2*, 662–672. (b) Miura, Y.; Satoh, K.; Kamigaito, M.; Okamoto, Y.; Kaneko, T.; Jinnai, H.; Kobukata, S. *Macromolecules* **2007**, *40*, 465–473.

(18) Wakioka, M.; Baek, K.-Y.; Ando, T.; Kamigaito, M.; Sawamoto, M. *Macromolecules* **2002**, *35*, 330–333.

(19) (a) Asandei, A. D.; Percec, V. *J. Polym. Sci., Part A: Polym. Chem.* **2001**, *39*, 3392–3418. (b) Percec, V.; Popov, A. V.; Ramirez-Castillo, E.; Monteiro, M.; Barboiu, B; Weichold, O; Asandei, A. D.; Mitchell, C. M. *J. Am. Chem. Soc.* **2002**, *124*, 4940–4941. (c) Percec, V.; Guliashvili, T.; Ladislaw, J. S.; Wistrand, A.; Stjerndahl, A.; Sienkowska, M. J.; Monteiro, M. J.; Sahoo, S. *J. Am. Chem. Soc.* **2006**, *128*, 14156–14165.

(20) Satoh, K.; Mizutani, M.; Kamigaito, M. *Chem. Commun.* **2007**, 1260–1262.

(21) (a) Fréchet, J. M. J.; Henmi, M.; Gitsov, I.; Aoshima, S.; Leduc, M. R.; Grubbs, R. B. *Science* **1995**, *269*, 1080–1083. (b) Hawker, C. J.; Fréchet, J. M. J.; Grubbs, R. B.; Dao, J. *J. Am. Chem. Soc.* **1995**, *117*, 10763–10764. (c) Simon, P. F. W.; Radke, W.; Müller, A. H. E. *Macromol. Rapid Commun.* **1997**, *18*, 865–873. (d) Müller, A. H. E.; Yan, D.; Wulkow, M. *Macromolecules* **1997**, *30*, 7015–7023. (e) Yan, D.; Müller, A. H. E.; Matyjaszewski, K. *Macromolecules* **1997**, *30*, 7024–7033. (f) Yan, D.; Zhou, Z.; Müller, A. H. E. *Macromolecules* **1999**, *32*, 245–250. (g) Gao, C.; Yan, D. *Prog. Polym. Sci.* **2004**, *29*, 183–275.

(22) (a) Marvel, C. S.; Chambers, R. R. *J. Am. Chem. Soc.* **1948**, *70*, 993–998. (b) Kobayashi, E.; Ohashi, T.; Furukawa, J. *Makromol. Chem.* **1986**, *187*, 2525–2533. (c) Kobayashi, E.; Obata, T.; Aoshima, S.; Furukawa, J. *Polymer Journal* **1990**, *22*, 803–813. (d) Klemm, E.; Sensfuss, S.; Holfter, U.; Schütz, H. *Makromol. Chem.* **1990**, *191*, 2403–2411. (e) Sato, E.; Yokozawa, T.; Endo, T. *Macromolecules* **1993**, *26*, 5187–5191.

(23) (a) Nagashima, H.; Wakamatsu, H.; Itoh, K.; Tomo, Y.; Tsuji, J. *Tetrahedron Lett.* **1983**, *24*, 2395–2398. (b) Iritani, K.; Yanagihara, N.; Utimoto, K. *J. Org. Chem.* **1986**, *51*, 5501–5503. (c) Hayes, T. K.; Villani, R.; Weinreb, S. M. *J. Am. Chem. Soc.* **1988**, *110*, 5533–5543. (d) Phelps, J. C.; Bergbreiter, D. E.; Lee, G. M.; Villani, R.; Weinreb, S. M. *Tetrahedron Lett.* **1989**, *30*, 3915–3918. (e) Nagashima, H.; Seki, K.; Ozaki, N.; Wakamatsu, H.; Itoh, K.; Tomo, Y.; Tsuji, J. *J. Org. Chem.* **1990**, *55*, 985–990. (f) Pirrung, F. O. H.; Steeman, W. J. M.; Hiemstra, H.; Speckamp, W. N.; Kaptein, B.; Boesten, W. H. J.; Schoemaker, H. E.; Kamphuis, J. *Tetrahedron Lett.* **1992**, *33*, 5141–5144. (g) De Campo, F.; Lastécouères, D.; Verlhac, J.-B. *Chem. Commun.* **1998**, 2117–2118. (h) De Campo, F.; Lastécouères, D.; Vincent, J.-M.; Verlhac, J.-B. *J. Org. Chem.* **1999**, *64*, 4969–4971. (i) De Campo, F.; Lastécouères, D.; Verlhac, J.-B. *J. Chem. Soc., Perkin Trans. 1* **2000**, *4*, 575–580. (j) Clark, A. J. *Chem. Soc. Rev.* **2002**, *31*, 1–11.

(24) (a) Ando, T.; Kamigaito, M.; Sawamoto, M. *Macromolecules* **2000**, *33*, 5825–5829. (b) Watanabe, Y.; Ando, T.; Kamigaito, M.; Sawamoto, M. *Macromolecules* **2001**, *34*, 4370–4374.

(25) (a) Ando, T.; Kamigaito, M.; Sawamoto, M. *Macromolecules* **1997**, *30*, 4507–4510. (b) Matyjaszewski, K.; Wei, M.; Xia, J.; McDermott, N. E. *Macromolecules* **1997**, *30*, 8161–8164. (c) Uchiike, C.; Terashima, T.; Ouchi, M.; Ando, T.; Kamigaito, M; Sawamoto, M. *Macromolecules* **2007**, *40*, 8658–8662.

(26) Xia, J.; Matyjaszewski, K. *Macromolecules* **1997**, *30*, 7697–7700.

(27) Queffelec, J.; Gaynor, S. G.; Matyjaszewski, K. *Macromolecules* **2000**, *33*, 8629–8639.

(28) Jakubowski, W.; Matyjaszewski, K. *Macromolecules* **2005**, *38*, 4139–4146.

(29) Jakubowski, W.; Min, K.; Matyjaszewski, K. *Macromolecules* **2006**, *39*, 39–45.

(30) Satoh, K.; Aoshima, H.; Kamigaito, M. *J. Polym. Sci., Part A: Polym. Chem.* **2008**, *46*, 6358–6363.

(31) (a) Detrembleur, C.; Mazza, M.; Halleux, O.; Lecomte, Ph.; Mecerreyes, D.; Hedrick, J. L.; Jérôme, R. *Macromolecules* **2000**, *33*, 14–18. (b) Lenoir, S.; Riva, R.; Lou, X.; Detrembleur, Ch.; Jérôme, R.; Lecomte, Ph. *Macromolecules* **2004**, *37*, 4055–4061.

(32) Hamasaki, S.; Kamigaito, M.; Sawamoto, M. *Macromolecules* **2002**, *35*, 2934–2940.

MA802067C